$Cu_{1.1}V_4O_{11}$: A New Positive Electrode Material for Rechargeable Li Batteries

M. Morcrette,*,† P. Martin,† P. Rozier,‡ H. Vezin,§ F. Chevallier,† L. Laffont,† P. Poizot,† and J.-M. Tarascon†

LRCS, Université de Picardie Jules Verne, 33 rue Saint-Leu, 80039, Amiens, France, CEMES, CNRS, BP 4347, 31055 Toulouse Cedex 4, France, and LCOM, CNRS UMR 8009 Bat C4 59655 Villeneuve d'Ascq Cedex, France

Received July 29, 2004. Revised Manuscript Received October 4, 2004

A new copper vanadate $Cu_{1.1}V_4O_{11}$ phase has been isolated by both chemical and electrochemical removal of Cu from the mother $Cu_{2.33}V_4O_{11}$ phase, and its electrochemical performance in Li cells has been studied. The removal of copper was shown to occur in a topotactic manner, resulting in a stacking of $[V_4O_{11}]_n$ layers linked by differently coordinated copper ions. This new phase reversibly reacts with 5 Li, leading to a capacity of about 260 mAh/g, through a process involving a reversible displacement reaction entailing to the growth/disappearance of Cu dendrites. However, in contrast to what was observed for $Cu_{2.33}V_4O_{11}$, this reversible copper extrusion/insertion process was shown neither to involve all of the Cu atoms (solely 0.8 out of the 1.1) nor lead to an amorphization of the electrode in its discharged sate. Structural considerations are put forward to account for such observed differences.

Introduction

Rechargeable Li-ion batteries are today standing as the most accepted technology to assist in the development of portable electronic devices. Yet, as new applications are coming on the scene, they fall short of meeting technological demands, hence, the sorely needed help to improve the existing Li-technologies by either acting on electrodes/electrolytes materials or searching for new concepts based on Li-driven conversion or displacement reactions.

Currently, layered structures oxides ($LiMO_2$ with M = Co, Ni), which exhibit good topotactic insertion/deinsertion properties, are mainly used as positive electrodes in Li-ion cells, while vanadates such as V_2O_5 or LiV_3O_8, which display capacities as large as 300 mAh/g at an average potential of 3 V, have emerged as promising positive electrodes for Li polymer-type batteries that are foreseen as possible candidates for automotive applications. In parallel, numerous studies are still focusing on the Li-containing three-dimensional framework structures such as the spinel ($LiMn_2O_4$) or olivine ($LiFePO_4$) phases for costs and environmental reasons or have been occasionally dealing in the past with insertion materials containing, besides Li^+, another mobile cation such as Cu^+ within the structure (e.g., $LiCuVO_4$), hoping that the mobile ions will help in achieving a high rate electrode material.[1]

Searching for other insertion electrodes, we recently isolated a new layered electrode material,[2] $Cu_{2.33}V_4O_{11}$, built up of $[V_4O_{11}]_n$ layers linked together by the copper ions but with no evident empty crystallographic sites to host lithium ions, which electrochemically react with Li in an unusual and spectacular way leading to a sustainable reversible capacity of 270 mAh/g (Figure 1a). More specifically, mechanistic studies have shown that the reaction entails a reversible Li-insertion/extrusion process leading to the growth/disappearance of Cu dendrites with a concomitant reversible amorphization/crystallization of the initial electrode material. We further studied the redox properties of such a compound in nonaqueous media and found as reported herein that $Cu_{2.33}V_4O_{11}$ can be both chemically and electrochemically oxidized to lead to a new phase $Cu_{1.1}V_4O_{11}$ that can reversibly react with 5 Li per formula unit through a Li-driven copper extrusion process.

Experimental Section

$Cu_{2.33}V_4O_{11}$ powders, prepared according to the literature[3] by reacting stoichiometric amounts of Cu_2O, V_2O_5, and V_2O_4 oxides at 540 °C under vacuum, were used as the precursor material to conduct the present study.

Powder purity and crystallinity were examined by X-ray diffraction (XRD), with a Scintag diffractometer operating in Bragg−Brentano geometry with a Cu Kα radiation, or unless otherwise specified by a Siemens D8 diffractometer using Co Kα radiation, and equipped with a PSD (position sensitive detector). The precursor $Cu_{2.33}V_4O_{11}$ powders were found to be single-phase with monoclinic lattice parameters (a = 15.309 Å, b = 3.610 Å, c = 7.355 Å, and β = 101.84°) similar to those previously reported. The charge distribution between the different Cu and V cations within the precursor phase was determined by analytical chemistry, titration techniques, to be $Cu^{+}_{1.2}Cu^{2+}_{1.1}V^{5+}_{2.56}V^{4+}_{1.44}O_{11}$, in good agreement with previous structural refinement and XPS measurements.[4]

* Corresponding author. E-mail: mathieu.morcrette@sc.u-picardie.fr.
† Université de Picardie Jules Verne.
‡ CEMES, CNRS.
§ LCOM, CNRS.

(1) Kanno, R.; Takeda, Y.; Hasegawa, M.; Kawamoto, Y.; Yamamoto, O. *J. Solid State Chem.* **1991**, *94*, 319.
(2) Morcrette, M.; Rozier, P.; Dupont, L.; Mugnier, E.; Sannier, L.; Galy, J.; Tarascon, J. M. *Nat. Mater.* **2003**, *2*, 755−761.
(3) Rozier, P.; Satto, C.; Galy, J. *Solid State Sci.* **2000**, *2*, 595−605.

10.1021/cm040181u CCC: $30.25
Published on Web 12/29/2004

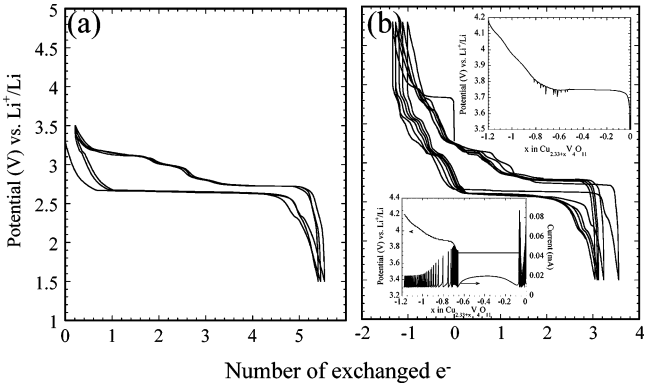

Figure 1. Room-temperature potential composition curve of a $Cu_{2.33}V_4O_{11}$/Li cell cycled in the 1.5−3.5 V voltage window at a C/5 rate (a) and of a $Cu_{2.33}V_4O_{11}$/Li cell first charged (to remove some copper) and then cycled at a C/5 rate in the 1.5−4.8 V voltage window (b). The top inset in (b) shows the presence of voltage spikes during the copper removal process. The PITT trace collected during the first charge of oxielectrochemical removal of Cu from the first inset as shown in the inset of a $Cu_{2.33}V_4O_{11}$/Li cell is shown as the bottom inset of part b (C/100 regime).

The powder morphology and composition were investigated by scanning electron microscopy (SEM) with a Philips XL 30 field emission gun (FEG), coupled to an Oxford Link instrument for energy-dispersive X-ray spectroscopy (EDS). They consist of 1000−2000 Å well-crystallized $Cu_{2.33}V_4O_{11}$ particles having a Cu/V ratio of 0.58 as separately confirmed by atomic absorption analysis. Besides, a Tecnaï F20 ST transmission electron microscope, equipped with EDS analysis, was used to conduct our TEM investigations on the chemically/electrochemically oxidized/reduced Cu−V−O samples.

The EPR spectra were recorded on Bruker Elexys E580E operating at 9 GHz and 100 kHz modulation frequencies. The spectra were recorded at room temperature with 5 mW microwave power and 5 G amplitude modulation. The EPR simulation spectrum was performed with the Bruker WinSimfonia software.

The electrochemical cells were performed in Swagelok-type cells assembled in an argon-filled dry box, using Li metal as the negative electrode, and a Whatman GF/D borosilicate glass fiber sheet, saturated with a 1 M $LiPF_6$ in ethylene carbonate (EC), dimethyl carbonate (DMC) (1:1 in weight) as the electrolyte. A 1 cm^2, 75 μm-thick composite electrode disk containing 10−15 mg of $Cu_{2.33}V_4O_{11}$, or a powder electrochemically/chemically mixed with 15% of carbon SP (black carbon from MM, Belgium), and made according to Bellcore's plastic Li-ion technology,[5] was used as the positive electrode. The lithium reactivity was monitored with a "VMP" potentiostat/galvanostat (Biologic S.A., Claix, France), operating in a galvanostatic mode. In-situ X-ray diffraction electrochemical cells assembled similarly to our Swagelok cell[6] but having a beryllium window as the current collector on the positive side, were placed on the same D8 diffractometer as above and were also connected to the Mac-Pile system for successive charge/discharge cycles.

Results and Discussion

Electrochemical Synthesis of $Cu_{1.1}V_4O_{11}$. A $Cu_{2.33}V_4O_{11}$|1 M $LiPF_6$|Li cell was initially charged up to a cutoff voltage of 4.8 V, and then cycled between 4.8 and 1.5 V. Although no Li was initially present in our electrode material, we noted the occurrence of an oxidation process (Figure 1b).

Once the current is applied, the 3.3 V initial cell voltage sharply reaches a 3.75 V plateau, whose length corresponds to a capacity of 0.7 e^-, and then smoothly rises up to 4.0 V over a Δx of 0.5 e^-, leading to an overall faradic process involving 1.2 e^-. Purely coincidentally or not, such a number (e.g., 1.2 e^-) corresponds, within the accuracy of the measurement, to the number of monovalent Cu^+ ions present in the precursor phase. To further clarify this point, we have performed the PITT (potentiostatic intermittent titration technique[7]) measurement (Figure 1b, inset). Besides highlighting the removal of copper in a two-step process, the experiment did confirm the capability to remove up to 1.2 e^-. Such a finding strongly suggests that, through the charging process of a $Cu_{2.33}V_4O_{11}$/Li cell, the monovalent copper ions known to be more mobile than the divalent Cu^{2+} are released from the $Cu_{2.33}V_4O_{11}$ electrode while V^{4+} ions are oxidized, with the overall result being the formation of a new "$Cu_{1.1}V_4O_{11}$" phase.

As an attempt to validate such a scenario, the electrochemically oxidized material recovered from a fully charged $Cu_{2.33}V_4O_{11}$/Li cell was washed with DMC and dried prior to being investigated by EDS, HRTEM, and X-ray measurements. EDS analysis confers to the oxidized material a $Cu_{1.1}V_4O_{11}$ chemical composition, while microscopy studies indicate a well-crystallized material as witnessed by the HRTEM image (Figure 2), which clearly shows the $[V_4O_{11}]_n$ layers with still some copper between them. Finally, the X-ray powder pattern of the oxidized material shows similarities to that of the parent $Cu_{2.33}V_4O_{11}$ (Figure 3), indicating that the extraction of copper ions is made without drastic structural modifications. It could indeed be indexed on the basis of a monoclinic unit cell with $a = 15.27$ (2) Å, $b = 3.45$ (1) Å, $c = 7.21$ (1) Å, and $\beta = 105.0$ (2)° as compared to $a = 15.31$ Å, $b = 3.61$ Å, $c = 7.35$ Å, and $\beta = 101.84°$ for $Cu_{2.33}V_4O_{11}$. Such changes in lattice parameters are not fortuitous but bear fruitful information. Besides the increase in the monoclinic angle β, it results that the copper extraction induces a slight decrease in the *a*-axis as compared to a larger one for the *b* and *c* cell parameters. So as Cu^+ ions are removed from the phase, the vanadium is oxidized, leading to less negatively charged and therefore less repulsive $[V_4O_{11}]_n^{\delta-}$ layers so that the layers can get closer together, consistent with the observed decrease in the *c*-axis. Such a decrease coupled with an increase in the monoclinic angle β strongly suggests a gliding of the layers as we move from the $Cu_{2.33}$ to the $Cu_{1.1}V_4O_{11}$ phase. In counterpart, the slight decrease in the *a* parameter, related to the length of the $[V_4O_{11}]_n$ layer, could indicate a puckering of the layers. Finally, the *b* cell parameter being related to the VO_6 octahedra periodicity in a layer, its decrease can simply be associated with the increase amount of V^{5+} during the oxidative process, because of the smaller length of V^{5+}−O bonds in comparison to V^{4+}−O bonds, V^{5+} having a smaller ionic radii than V^{4+}.

(4) Rozier, P.; Galy, J.; Chelkowska, G.; Kooh, H.-J.; Whangbo, M.-H. *J. Solid State Chem.* **2002**, *166*, 382−388.
(5) Tarascon, J. M.; Gozdz, A. S.; Schmutz, C.; Shokoohi, F.; Warren, P. *Solid State Ionics* **1996**, *86*−*88*, 49−54.
(6) Morcrette, M.; Chabre, Y.; Vaughan, G.; Amatucci, G.; Leriche, J.-B.; Patoux, S.; Masquelier, C.; Tarascon, J.-M. *Electrochim. Acta* **2002**, *47*, 3137−3149.
(7) Chabre, Y. In *Chemical Physics of Intercalation*; Bernier, P., Ed.; Plenum: New York, 1993.

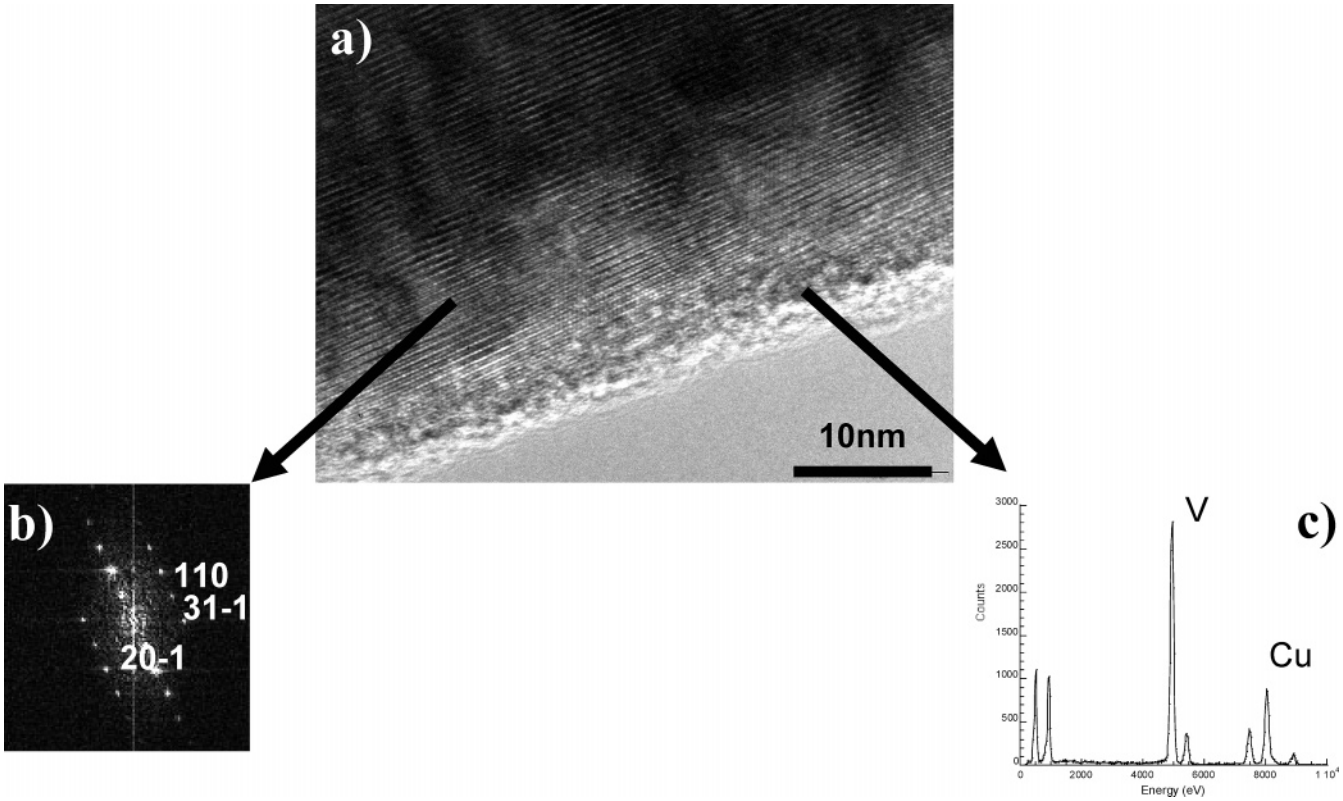

Figure 2. TEM study realized on a "$Cu_{1.1}V_4O_{11}$" sample. (a) HRTEM image showing that the material is still crystallized. The observed contrast evidences that some copper is still stacked between the V_4O_{11} layers. (b) The corresponding SAED pattern could be indexed with the $Cu_{1.1}V_4O_{11}$ cell parameters determined from X-ray diffraction and correspond to a [1-12]* zone axis. (c) EDS analysis realized on the observed region; the quantification of the vanadium copper ratio gives a value close to 4, which is in good agreement with the theoretical value.

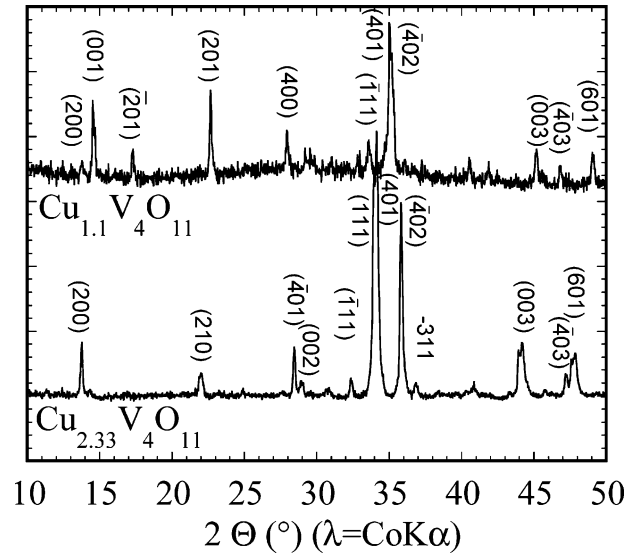

Figure 3. X-ray diffraction pattern of the $Cu_{1.1}V_4O_{11}$ phase; this phase is indexed on the basis of a monoclinic unit cell with $a = 15.27(2)$ Å, $b = 3.45(1)$ Å, $c = 7.21(1)$ Å, and $\beta = 105.0(2)°$. The $Cu_{2.33}V_4O_{11}$ phase is also reported for comparison.

Turning back to the $Cu_{2.33}V_4O_{11}$/Li cell charging voltage profile, it is worth stressing that it was not as smooth as usual, but rather noisy and showing a few voltage spikes (Figure 1b, inset) indicative of a few electrical shorts developing through the charging process. Interestingly, voltage spikes are not unfamiliar to the battery community because they have long been observed in rechargeable Li batteries and ascribed to the formation and partial melting of Li dendrites. Thus, the legitimate question was whether the origin of such voltage spikes could be linked to the release of Cu^+ ions into the electrolyte. To shed some light on this issue, we checked by EDX analysis the Li negative electrode recovered from a $Cu_{2.33}V_4O_{11}$/Licell that was charged up to 4.8 V vs Li^+/Li, and we revealed the presence of metallic copper on its surface, implying that the Cu ions released from the $Cu_{2.33}V_4O_{11}$ positive electrode, because of the migration together with the mass transfer phenomenon, move through the electrolyte toward the Li electrode where they are reduced into metallic copper, forming dendrites that are most likely responsible for the observed voltage spikes. Unfortunately, because of the presence of metallic Cu poisoning the Li negative electrode surface during the charging process, the cell was found to perform very poorly on the following discharge, preventing reliable studies regarding the electrochemical performance of the newly synthesized "$Cu_{1.1}V_4O_{11}$" electrode material vs Li in Li cells.

Chemical Synthesis of $Cu_{1.1}V_4O_{11}$. To circumvent such a difficulty and enable the synthesis of large amounts of $Cu_{1.1}V_4O_{11}$ powders, we decided to mimic the electrochemical oxidation process using a chemical one (as described below), which consists of using 1 M NO_2BF_4 acetonitrile solution as the oxidizing agent; the NO_2^+/NO_2 couple was the active redox couple, while the BF_4^- ions solely act as spectators.

$$Cu_{2.33}V_4O_{11} + xNO_2BF_4 \xrightarrow[12\ h]{\text{acetonitrile}} Cu_{2.33-x}V_4O_{11} + xCu^+ + xBF_4^- + xNO_2\uparrow$$

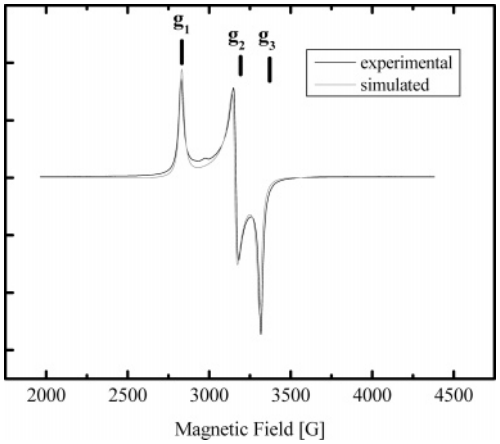

Figure 4. Experimental and simulated EPR spectra of fully oxidized $Cu_{1.1}V_4O_{11}$ recorded at room temperature.

The experiment was conducted at room temperature in an argon dry box by placing in a glass vessel 1 g of $Cu_{2.33}V_4O_{11}$ powder, and by pouring over a 200 mL acetonitrile solution containing 2 g of dissolved NO_2BF_4 (i.e., around 3 times excess as compared to stoichiometric conditions). Within a few minutes after the magnetic agitation was turned on, the colorless solution progressively turned greenish, implying the release of copper ions and hence the advancement of the oxidation reaction. By monitoring, through atomic absorption analysis, the amount of copper in the reacting solution as a function of the steering time, and by subsequent solution withdrawals, we noted that the copper content was no longer evolving after 7 days of reacting time. Thus, afterward, the 7 days reacting solution mixture was filtered, and the recovered resulting powder was washed and dried prior to being characterized for its structure and composition. Such chemically made samples will be denoted hereafter as CM as opposed to EM for the ones electrochemically made.

Such analysis did not bear any surprise. The X-ray powder pattern of the CM sample was found to perfectly superimpose with that of the EM sample. Its Cu/V ratio, as deduced by EDX analysis, was shown, within the accuracy of the measurements, to be equal to 0.30 as compared to 0.28 for the EM sample, thus enabling us to assign to this new phase a general formula $Cu_{1.1}V_4O_{11}$ that was further confirmed by chemical analysis. Because of the charge neutrality argument, such a formula implies that we could either have the coexistence of (1) V^{4+}, V^{5+}, and Cu^{2+} ($Cu^{2+}{}_{1.1}V^{4+}{}_{0.3}V^{5+}{}_{3.7}O_{11}$), (2) of V^{5+} together with a mixture of Cu^{2+} and Cu^{+} ($Cu_{0.9}{}^{2+}Cu^{+}{}_{0.2}V^{5+}{}_4O_{11}$), or a mixture of both. To sort out between these different possibilities, we have performed EPR measurements of the fully oxidized phase, because $Cu^{2+}(d^9)$ and $V^{4+}(d^1)$ ions are EPR actives, while Cu^{+} (d^{10}) and V^{5+} (d^0) are not. The EPR spectrum collected on the CM $Cu_{1.1}V_4O_{11}$ phase (Figure 4) displays the fully oxidized material; it shows the signature expected for an octahedral coordinated Cu^{2+} Jahn Teller ion with no traces of V^{4+}. The g anisotropy is well resolved and allows us to determine the values of the three g_1, g_2, and g_3 factors equal to 2.39, 2.14, and 2.038, respectively. Simulation of the spectrum was performed and provides a good agreement with the experimental spectrum. Through a fitting of the collected spectra, we could deduce that the single electron sits on the d_{z2} orbital, which implies a compression of the octahedra along the c-axis and an expansion within the basal plane.

Overall, the EPR data (i.e., the absence of V^{4+}) imply the following charge balance ($Cu^{2+}{}_{0.9}Cu^{+}{}_{0.2}V^{5+}{}_4O_{11}$) for our newly synthesized phase leading to the expectation that 1.4 e^- (0.2 Cu^{2+} + 1 Cu^{+}) should be removed from $Cu_{2.33}V_4O_{11}$ upon electrochemical oxidation. At first sight, this number drastically conflicts with the electrochemical titration result described earlier in the text (PITT) that indicates the removal of solely 1.2 e^- (i.e., 1.2 Cu^{+}) from $Cu_{2.33}V_4O_{11}$ upon oxidation. Therefore, we believe that they can be reconciled by simply considering the possibility of an internal redox process between Cu^{2+} and V^{4+}. Within such a scenario, the removal of 1.2 Cu^{+} from $Cu_{2.33}V_4O_{11}$ will produce a $Cu_{1.1}V_4O_{11}$ phase having the hypothetical "$Cu^{2+}{}_{1.1}V^{5+}{}_{3.8}V^{4+}{}_{0.2}O_{11}$" charge balance that will instantaneously, through the internal reduction of Cu^{2+} by V^{4+}, lead to the following charge repartition $Cu^{2+}{}_{0.9}Cu^{+}{}_{0.2}V^{5+}{}_4O_{11}$ in agreement with the EPR data. Thus, by way of summary, the electrochemically/chemically driven removal of Cu from $Cu_{2.33}V_4O_{11}$ can be described according to the global reaction listed below:

$$Cu_{1.2}{}^{+}Cu_{1.1}{}^{2+}V_{2.56}{}^{5+}V_{1.44}{}^{4+}O_{11} \rightarrow Cu_{0.9}{}^{2+}Cu_{0.2}{}^{+}V_4{}^{5+}O_{11} + 1.2\ Cu^{+} + 1.2\ e^{-}$$

Finally, the moisture and thermal stability of the CM $Cu_{1.1}V_4O_{11}$ powders were investigated. The phase was found to be thermally stable up to temperatures of about 600 °C, because no anomaly either in the TGA curve or in the X-ray powder pattern of the heated sample was observed. However, we noted a slight evolution of the X-ray powder pattern of the $Cu_{1.1}V_4O_{11}$ phase when kept in ambient air for about 1 month, indicative of the occurrence of some chemical redox reaction. Knowing that such a phase forms at about 4 V vs Li, it is quite likely that such a compound oxidizes water so that the formation of the reduced phase $Cu_{1.1}V_4O_{10}OH$ was suspected and confirmed by the low-temperature H_2O (<100 °C) weight loss in the TGA measurements.

Electrochemical Insertion of Li into $Cu_{1.1}V_4O_{11}$. The CM $Cu_{1.1}V_4O_{11}$ powders were processed into plastic laminates according to Bellcore's technology, and the same 68/12/20 weight ratio of active material/carbon black/and PVDF-HFP was used, respectively. $Cu_{1.1}V_4O_{11}$/Li cells were then assembled and tested for their room-temperature electrochemical performances upon cycling as a function of various discharge/charge rates and cycling potential windows. Figure 5 shows a typical potential−composition trace for a $Cu_{1.1}V_4O_{11}$/Li cell cycled between 1.5 and 4.5 V at a C/5 rate. During the first discharge, the potential initially drops noncontinuously in a stepwise fashion down to $x = 1.8$ to reach a plateau at 2.6 V having a capacity of about 2.6 Li. Finally, an extra 0.7 Li can be reacted as the potential reaches 1.5 V. Upon recharge, most of the 5.1 uptake lithium can be removed, leading to reversible capacities ranging from 230 to 260 mAh/g of $Cu_{1.1}V_4O_{11}$ as compared to 250−270 mAh/g for the precursor $Cu_{2.33}V_4O_{11}$ phase. The subsequent charge/discharge curves were found to superimpose, implying a steady capacity retention as reported in Figure 5, inset, for at least the first few tens of cycles whatever the cycling rate

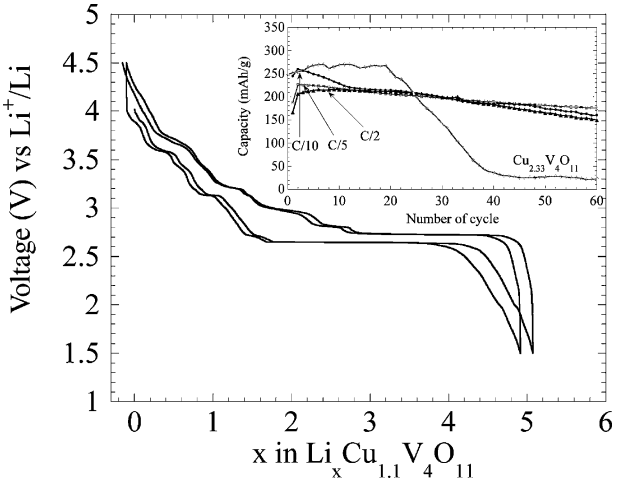

Figure 5. Room-temperature voltage−composition profile of a chemically prepared $Cu_{1.1}V_4O_{11}$/Li cell cycled in the 1.5−4.5 V window at a regime of C/5.

(C/2, C/5, or C/10). The capacity was then shown to smoothly and continuously decrease over the subsequent cycles in contrast to that of $Cu_{2.33}V_4O_{11}$/Li cells that abruptly dropped after 20 cycles. Because of the post-mortem investigation of cycled $Cu_{2.33}V_4O_{11}$/Li and $Cu_{1.1}V_4O_{11}$ cells by scanning electron microscopy that has revealed the presence of copper deposits at the Li-negative electrode, the origin of the measured limited capacity retention is most likely nested in both cases in the poisoning of the Li negative electrode by Cu. If so, the copper content being greater in the $Cu_{2.33}V_4O_{11}$ phase than in the $Cu_{1.1}V_4O_{11}$, one would expect the poisoning effect, and therefore the capacity decay, to be greater for the former than for the latter, as observed. However, for such a comparison to be meaningful, the mechanisms of the Li-insertion process in both compounds must be similar (i.e., it entails the release and uptake of copper).

In Situ X-ray Diffraction. To check this point, an in-situ X-ray electrochemical $Cu_{1.1}V_4O_{11}$/Li cell was assembled, placed in a D8 diffractometer, and discharged/charged at low current density (1 Li in 4 h). The most prominent X-ray powder patterns collected during the discharge are reported in Figure 6a. As a $Cu_{1.1}V_4O_{11}$/Li cell was discharged, we initially observed up to $x = 0.7$ a progressive splitting of the main (401) and (402) Bragg peaks located at $2\Theta = 35.2°$ (zoomed region in Figure 6a) that led to the phase $Li_{0.7}Cu_{1.1}V_4O_{11}$ that was refined with lattice parameters equal to $a = 15.38$ Å, $b = 3.40(1)$ Å, $c = 7.30(1)$ Å, and $\beta = 105.5(2)°$, and that will be referred to later as the A phase. Upon further increasing x, some extra peaks located at 2Θ equal to 34° and 36° appear and grow at the expense of the ones located around $2\Theta = 35.2°$ to become unique for $x = 0.9$. These peaks were found to correspond to a new phase (denoted B), whose domain of solid solution ranges from 0.9 to about 1.3, and that can be indexed in a monoclinic cell with the following lattice parameters $a = 15.39$ Å, $b = 3.65(1)$ Å, $c = 7.20(1)$ Å, and $\beta = 101.25°$. The large decrease in the monoclinic angle β (105.5° to 101.1°) in going from the A to B phase is indicative of a gliding of the $[V_4O_{11}]_n$ layers, as one could expect from such a layered structure. It is worth noting that the lattice parameters of the B phase, whose composition is $Li_{1.3}Cu_{1.1}V_4O_{11}$ (within the accuracy of the electrochemical titration), are very close to those of $Cu_{2.33}V_4O_{11}$. This will suggest that Li^+ ions take the place of Cu^+ with the structure of $Cu_{1.1}V_4O_{11}$. As the amount of reacted Li exceeds 1.3, we note, among others, the rapid growth of one Bragg peak located at 50.7° and indicative of the growth of metallic copper. Because of the overall decrease in intensity of the X-ray powder patterns, it is difficult to identify/index the phases that coexist, thus limiting the establishment of the $Li_xCu_yV_4O_{11}$ room-temperature phase diagram to a visual scrutinizing of the X-ray powder patterns so as to spot two-phase versus single-phased domains. Along that line, for $x = 2.4$, the composite appears as a composite consisting of Cu metal coexisting with a C-phase. From $x = 2.4$ to 4.3, the flat and large plateau is characteristic of a multiphase process, but in the same manner as before, we never succeeded in clearly solving the structural

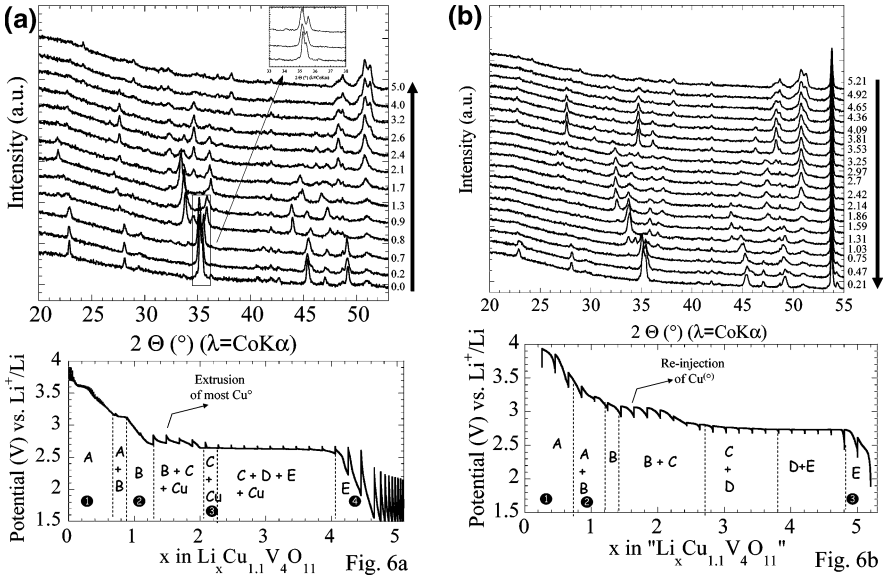

Figure 6. In-situ X-ray diffraction performed on a $Cu_{1.1}V_4O_{11}$/Li cell discharged (a) and charged (b) at a rate of 1 Li in 20 h. X-ray scans were collected for every inserted 0.2 Li with 30 min data acquisition times, but, for reasons of clarity, only some of the most relevant scans are reported. The electrochemical phase diagrams are reported below the in-situ X-ray patterns.

parameters of the "D" and "E" phases. Finally, it is worth noting that we measured a small increase in the Cu (111) peak during the reaction from the C to E phase.

Upon the charge process, the first E → D transition is nicely identified with the progressive appearance of a new set of peaks located at 28°, 35°, and 49° corresponding to the first plateau at 2.6 V. Note that we could not isolate such a D phase during the first cell discharge most likely because of kinetic limits. Suddenly, all of these peaks disappeared at the expense of the C phase with broad peaks at 33° that were also identified during the discharge. From $x = 3.4$ to $x = 1.8$, the (111) peak of metallic copper is totally washed out, in good agreement, so that only the Bragg peaks corresponding to the B phase, as previously identified, remain. Upon further delithiation, the B phase converts back to the A phase, so that the structure of the precursor phase $Cu_{1.1}V_4O_{11}$ is fully recovered with identical lattice parameters. Thus, at first, the overall process sounds identical to what has been observed during the Li-insertion/deinsertion process in $Cu_{2.33}V_4O_{11}$ (reversible Cu extrusion/insertion and conversion back to the well-crystallized precursor phase), with two noticeable differences being (1) a partial Cu exclusion of $Cu_{1.1}V_4O_{11}$ as compared to a full one of $Cu_{2.33}V_4O_{11}$ and (2) the existence of a crystallized material for the discharged $Cu_{1.1}V_4O_{11}$ electrode composite as compared to an amorphous one for the discharged $Cu_{2.33}V_4O_{11}$ electrode.

As an attempt to determine at which stage of the Li-insertion/deinsertion process the $Cu^{2+} \rightarrow Cu^{(0)}$ reduction was occurring, and whether all of the Cu^{2+} ions were involved, we further exploited the X-ray data in a manner similar to that for $Cu_{2.33}V_4O_{11}$. The exploitation was therefore not as straightforward, because the range of 2Θ activity for Cu appearance is masked by the growth of a few Bragg peaks of the main phase associated to Li-driven phase transitions. Therefore, one peak, the (111) copper peak located at $2\Theta = 50.7°$ appears relatively narrow and slightly perturbed from side peaks. Thus, we decided to use the intensity variation of this peak as a way to deduce the number of copper atoms released from $Cu_{1.1}V_4O_{11}$ as a function of the number of electrochemically reacted Li. To quantify such analysis of the X-ray powder patterns, and thus quantify the removed amount of copper atoms, a reference was needed. Because such an in-situ X-ray experiment was conducted on the same electrochemical X-ray cell as our previous in-situ X-ray study of $Cu_{2.33}V_4O_{11}$/Li cells, we decided to use the beryllium peaks as the internal reference for both experiments. More specifically, from the previously collected in-situ X-ray data on $Cu_{2.33}V_4O_{11}$, we simply determined the ratio of the Cu (111) peak intensity at its maximum over the *hkl* beryllium peak intensity and took this ratio as equal to 2.33 (i.e., equivalent to 2.33 Cu atoms). Because of such an assumption, the corresponding amount of copper associated with the growth of the Cu (111) peak during the discharge of CuV_4O_{11}/Li cells can be deduced by plotting the ratio Y defined by:

$$Y = [I_{Cu}{}^1/I_{Be}{}^1]/[I_{Cu}{}^0/I_{Be}{}^0]*2.33$$

where indices 1 and 0 represent the experiment realized on

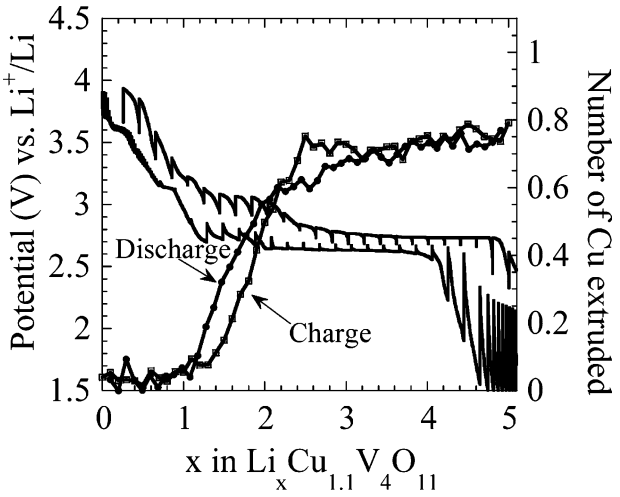

Figure 7. Room-temperature voltage composition in relation to the number of extracted copper calculated from the in-situ X-ray experiment (details are given in the text).

$Cu_{1.1}V_4O_{11}$ and $Cu_{2.33}V_4O_{11}$, respectively. Thus, we could assign to each scan the number of released copper atoms corresponding to a well-defined number x of inserted Li^+ ions. Interestingly, this number does not vary linearly with the inserted number of Li^+ (x) over the entire composition range but shows differentiated domains. Initially (Figure 7), the Li-insertion is associated to the reduction of some V^{5+} into V^{4+} and proceeds without any copper extrusion (slope 0) to lead to the phase previously denoted B. Upon further lithiation, the curve shows a linear variation with a slope of about 2, indicating that over this range of composition in Li (from $x = 1$ to $x = 2$) the number of inserted Li atoms is about twice greater than the number of extruded copper atoms as expected, based on the fact that within the precursor phase the Cu ions are divalent so that two electrons (e.g., 2 Li^+) are needed to reduce a Cu^{2+} ion. Beyond $x = 2.1$ and up to $x = 5$, the slope of the curve returns nearly to zero, leading to a calculated amount of removed copper atoms that does not exceed 0.15 to 0.2 and suggesting that over such a composition range the Li-insertion process is mainly associated with the reduction of V^{5+} to V^{4+}. Although caution should be exercised in overinterpreting the data, because of a nonstraightforward analytical process of the X-ray powder patterns, a nondisputable message conveyed from this graph resides in the fact that the amount of removed copper, even after complete electrochemical lithiation, does not exceed 0.75, implying an incomplete Li-driven copper extrusion process as compared to the complete one previously observed for $Cu_{2.33}V_4O_{11}$. Although the process was not complete, as for $Cu_{2.33}V_4O_{11}$, it is totally reversible, as witnessed by the superposition of the curve, corresponding to the number of reinserted copper atoms as function of the number of released Li atoms during the charging process, with that obtained during the discharging process. Finally, besides $x = 2.1$, the remaining 0.35 copper atoms in the fully lithiated $Li_xCu_{0.35}V_4O_{11}$ composite could act as a pillar between the $[V_4O_{11}]_n$ layers, then preserving the collapsing of the structure, so that the fully discharged composite will still be crystalline in contrast to the fully delithiated $Cu_{2.33}V_4O_{11}$ sample that was very disorganized, as we observed.

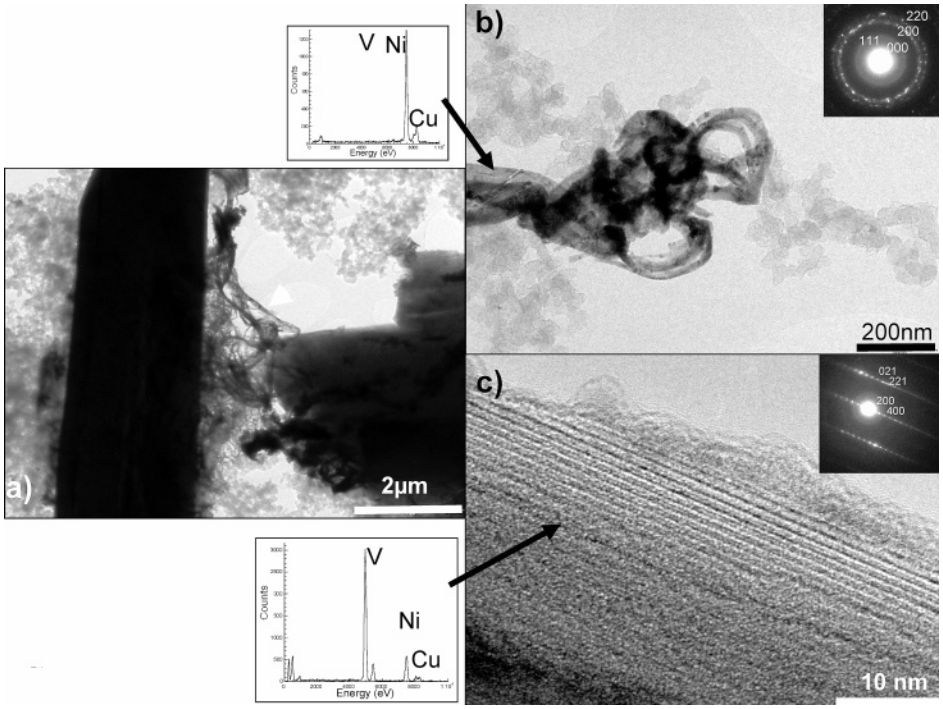

Figure 8. TEM study realized on the fully discharged "$Cu_{1.1}V_4O_{11}$" electrode. (a) Overall bright-field image showing dendrites (white arrows) coming out of the initial needle-shape particles. (b) Zoom on one of these dendrites with corresponding EDS analysis. Only nickel (coming to the MET grid) and copper signals are observed, showing that the dendrite is made of pure copper. This point was confirmed by the corresponding SAED pattern indexed with metallic copper cell parameters. (c) HRTEM image realized on the edge of the remaining needle. These needles are still crystallized according to the observed contrast showing $[V_4O_{11}]_n$ layers and to the corresponding punctual SAED pattern given in the inset. It is worth noting that the amorphous contrast observed on a part of the image is not intrinsic but is induced by the electron beam during observation at high magnification (amorphization under the beam). Quantification of EDS spectrum realized on the corresponding region leads to a Cu/V ratio equal to 0.125.

High-Resolution Electron Microscopy ex Situ Measurements. The evidence for the Li-electrochemically driven Cu-extrusion being given, questions remain concerning the details of the degree of completeness of the copper extrusion process as well as the morphology of the extruded copper. Is it dendritic as previously shown in the fully electrochemically discharged "$Cu_{2.33}V_4O_{11}$" electrodes versus lithium? To address these issues, we studied $Cu_{1.1}V_4O_{11}$ electrodes at various stages of the reduction and oxidation processes by means of high-resolution transmission electron microscopy (HRTEM). Here, we will only report results on the precursor (Figure 2), the totally (reduced) discharged (Figure 8), and the fully recharged (oxidized) electrode materials (Figure 9).

Bright-field images indicate that the CM electrode consists of 1000−2000 Å well-crystallized $Cu_{1.1}V_4O_{11}$ particles. For the fully reduced "$Li_5Cu_{1.1}V_4O_{11}$" sample, the bright-field image (Figure 8) shows that the initial particles transform into thick dark grains that are well crystallized, because a well-resolved SAED pattern could be collected. EDS analysis on such crystallites for Cu and V indicated a composition of "$Li_xCu_{0.5}V_4O_{11}$", which agrees well with the $Li_xCu_{0.3}V_4O_{11}$ composition indirectly determined by X-ray studies, and confirmed that the Cu extrusion process is solely partial. In addition, we observed the growth of filaments that were identified as copper dendrites from the collected SAED pattern (inset) recorded from the circled region, and this was confirmed by EDS analysis. It looks like, upon Li reduction of $Cu_{1.1}V_4O_{11}$, some of the incoming Li-ions are pushing the Cu ions out of the structure, leading to filamentary copper plus a well-crystallized Li−Cu−V−O phase. The HRTEM image of such an electrode reoxidized up to 4.5 V (Figure 9) shows that the Li−Cu−V−O + Cu composite electrode converts back to the original phase with the regrowth of well-crystallized $Cu_{1.1}V_4O_{11}$ platelets (Figure 9a and b) as deduced from an indexation of the ordered and well-defined diffraction spots of the corresponding collected SAED patterns, one of which is shown in Figure 9c.

EPR Measurements. Finally, in an attempt to exploit the Li-insertion process into this compound, and more specifically to better understand how it affects the acceptor Cu^{2+} and V^{5+} levels within the phase, we pursued EPR measurements on partially "$Li_xCu_{1.1}V_4O_{11}$" samples. More specifically, we investigated the $x = 0.5$, $x = 2$, and the fully lithiated samples (at 1.5 V). Because of the EPR activity of carbons, the electrodes were prepared carbon-free and reduced at a very low rate (1 Li in 100 h). Once the suitable x values were reached, the samples were washed with DMC, and then dried prior to being sealed in 4 mm quartz tubes.

The insertion of 0.5 Li into the precursor $Cu_{1.1}V_4O_{11}$ phase was found to provoke a drastic change of its EPR spectra (Figure 10a), with the loss of the well-resolved anisotropic signal, characteristic of an octahedral coordinated Cu^{2+} ion, at the expense of a 300 G broad signal. The transition from an anisotropic Cu^{2+} signal to an isotropic one having a partially resolved A_{Cu} hyperfine splitting constant of 80 G and $g = 2.01$ indicates a symmetry change distortion of the octahedron with an increase in the (d_{x2-y2}) character. For $x = 2$ (Figure 10b), the EPR trace contains both Cu^{2+} and V^{4+} signals with g values of 2.01 and 1.99, respectively. The Cu^{2+} signal becomes barely detectable as compared to the V^{4+} EPR signal. The onset of the V^{4+} signal, masked by the prominent Cu^{2+} signal in the $x = 0.5$ phase, was expected

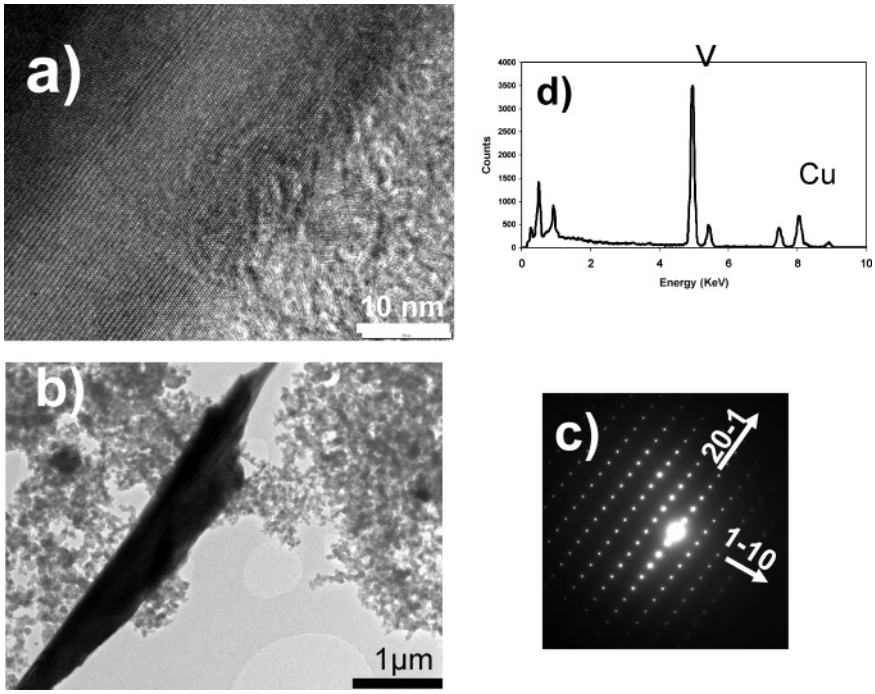

Figure 9. TEM study realized on the reoxidized material. (a) Enlarged HRTEM image of a region of the particle presented in (b), showing that the material is perfectly crystallized. Copper dendrites have disappeared. (c) According to the [112]* zone axis SAED pattern indexed with $Cu_{1.1}V_4O_{11}$ cell parameters and (d) to the quantitative analysis of the recorded EDS spectrum (V/Cu = 4), the conversion back to the original phase could be assumed.

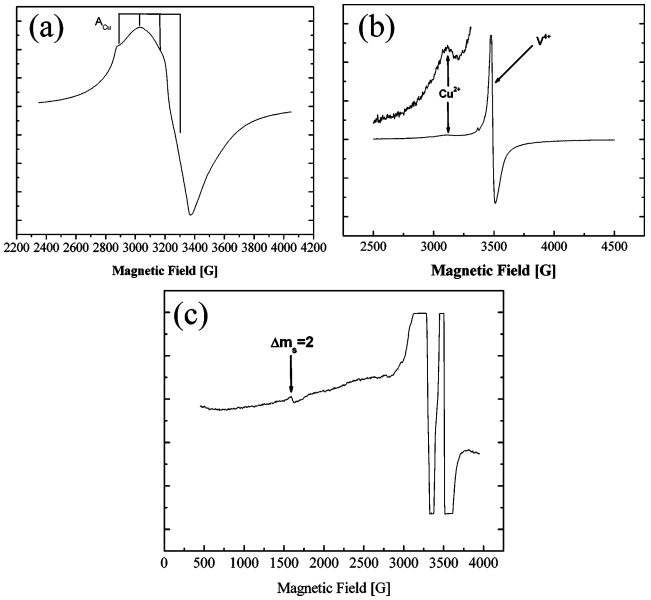

Figure 10. Experimental EPR spectra recorded at room temperature of $Cu_{1.1}V_4O_{11}$ electrode lithiated at different levels: (a) 0.5 Li, (b) 2 Li, and (c) fully discharged.

due to the Li electrochemical driven $V^{5+} \rightarrow V^{4+}$ reduction process. However, the weak intensity of the Cu^{2+} detected signal can be surprising, but the integral measurement as $\Delta H^2 \times I$ (ΔH is the line width peak to peak and I is the intensity of signal) yield a ratio Cu^{2+}/V^{4+} close to 1/1 with a smaller proportion of Cu^{2+} species. We should therefore recall that, as the Li-insertion proceeds from 0.5 to 2, there is a removal of 0.6 Cu atoms from the structure together with a drastic rearrangement of the parent phase, so that one can anticipate weaken Cu−Cu interactions because of both an increased structural disorder as well as a Li-driven matrix dilution effect. Finally, for the fully lithiated sample (Figure 10c), the EPR signal consists of components reminiscent of the presence of both V^{4+} and Cu^{2+} ions as observed for $x = 2$. Additionally in this lithiated sample, a new spectral feature is measured at half-field signal. This signal is the so-called $\Delta m_s = 2$ forbidden transition arising from the J exchange Hamiltonian term, whose origin is nested in electron−electron interaction via exchanging mechanism expressed as S1 × J × S2 where J is the exchange coupling constant. This signal arises from the population of a triplet state due to probable interactions between $V^{4+}-V^{4+}$, $Cu^{2+}-Cu^{2+}$, or $Cu^{2+}-V^{4+}$ species. The intensity of the $\Delta m_s = \pm 2$ transition as compared to the $\Delta m_s = \pm 1$ signal has been used for the determination of the magnitude of the interspin vector r in a wide variety of organic diradical, metal−metal dimers.[8−10] Such interspin vector distance can be determined using the following empirical formula:[10] relative intensity $= A/r^6$, where $A = (19.5 + 10.9\Delta g)(9.1/\nu)^2$. We have found a distance of 3.85 Å between the two paramagnetic centers. Therefore, in the absence of any structural details for such a fully delithiated sample, we cannot presently affect such a distance to any of the $V^{4+}-V^{4+}$, $Cu^{2+}-Cu^{2+}$, or $Cu^{2+}-V^{4+}$ interactions.

Conclusions

In short, we have reported the chemical synthesis of a new $Cu_{1.1}V_4O_{11}$ phase that can reversibly react with 5.1 Li at an average potential of 2.6 V through a mechanism involving at first sight a reversible extrusion and reinjection of Cu within the structure as for the recently reported $Cu_{2.33}V_4O_{11}$ electrode. However, through a careful study of the Li reactivity toward $Cu_{1.1}V_4O_{11}$ by means of an arsenal of in-

(8) Bencini, A.; Gatteschi, D. *Electron Paramagnetic Resonance of Exchange Coupled Systems*; Springer: Berlin Heidelberg, 1990; p 187.
(9) Eaton, S. S.; Eaton, G. R. *J. Am. Chem. Soc.* **1982**, *104*, 5002−5003.
(10) Coffman, R. E.; Pezeshk, A. *J. Magn. Reson.* **1986**, *70*, 21−33.

situ/semi in-situ X-rays, microscopy, and EPR measurements, we have spotted some consequent differences with (1) the preservation of the electrode crystallinity through all of the reversible process as opposed to an amorphization/recrystallization for the $Cu_{2.33}V_4O_{11}$ phase, and (2) a limitation of the copper extrusion process to only 0.75 of the 1.1 Cu atoms present in the phase while the 2.33 Cu atoms are involved in the parent phase, and a better capacity retention for $Cu_{1.1}V_4O_{11}$/Li cells as compared to $Cu_{2.33}V_4O_{11}$/Li. So a legitimate question deals with the origin of such differences.

A possible answer may be in structural considerations. Although the poor crystallinity of the samples did not allow us to solve exactly the structure of the extracted compound, we could, because of complementary electrochemical and EPR experiments, show that the copper-deficient phase, because of the puckering of the $[V_4O_{11}]_n$ layers along the *a*-axis combined with their gliding along the *c*-axis, can be described as a packing of $[V_4O_{11}]_n$ layers linked together by Cu^{2+} ions in octahedral surroundings. Such a surrounding differs from that of the Cu^{2+} ions in the parent phase $Cu_{2.33}V_4O_{11}$, which oscillates between tetrahedral−octahedral coordination sites, with the expectation of a weaker Cu−O bonding. Thus, because of the strengthening of the Cu−O bond in the $Cu_{1.11}V_4O_{11}$, the octahedrally coordinated Cu^{2+} ions could act as pillars, tightening the $[V_4O_{11}]_n$ layers together, hence explaining the partial Li-driven Cu extrusion/reinjection process encountered with his compound as compared to the full one experienced with $Cu_{2.33}V_4O_{11}$. By the same token, these strengthened Cu−O bonds are expected to limit the $[V_4O_{11}]_n$ layers rearrangement. The flexibility of the structure being restrained, a long-range order is maintained and is most likely responsible for the crystalline aspect of the fully discharge sample.

Energetically wise, such a Li-driven copper extrusion-process in $Cu_{1.1}V_4O_{11}$ can be understood in a structure having several acceptor Cu^{2+} and V^{5+} levels, and by assuming that the copper ones are those with the lowest energy, so that they will be reduced first leading to copper metal. Obviously, such a level positioning is directly linked to the material electronic band structure that is strongly dependent on the crystallographic structure. Because of the complex Li-driven structural changes, the cation energy levels can easily cross over so that we could easily swing between the reduction of Cu^{2+} or V^{5+}, hence, the need to launch some studies on the band structure calculations.

Finally, while quite spectacular with the appearance/disappearance of micrometer-size dendrites, a drawback of such electrodes operating on this Li-driven Cu extrusion−insertion process is their poor capacity retention, whose origin is nested in copper dissolution issues. As the Cu-based electrode is discharged, the incoming Li ions enter the structure and chase the Cu ions to the particle edge where they are reduced leading to copper nucleation and copper dendrite growth. Upon recharge, for the reaction to reversibly proceed, one must oxidize copper metal to produce Cu^{2+} ions in solution that will rapidly enter the structure. Because of the competing rate of the copper oxidation versus copper reinjection reactions, some of the copper ions can escape from the positive electrode to move toward the negative electrode where they will be reduced, limiting then the recharge process. Based on simple-minded extrapolation, we will simply expect that the extent of this copper dissolution process will scale with the number of Cu atoms involved in the reversible process, and therefore be higher for the $Cu_{2.33}V_4O_{11}$/Li cells as compared to the $Cu_{1.1}V_4O_{11}$/Li cells because the former involves the uptake removal of 2.33 Cu instead of 0.75 for the latter, in agreement with our experimental observations. We are presently studying various possibilities, by acting on either the electrode configuration and/or the particle coatings to minimize the copper migration in such cells.

Acknowledgment. We thank L. Dupont, D. Larcher, and F. Gillot for their useful technical discussions.

CM040181U